

The Catalytic Ammoxidation of Propylene over Bismuth Molybdate Catalyst

S. P. LANKHUYZEN, P. M. FLORACK,¹ AND H. S. VAN DER BAAN

Department of Chemical Technology, University of Technology, Eindhoven, The Netherlands

Received January 16, 1975; revised June 30, 1975

The continuous catalytic ammoxidation of propylene over the koechlinite phase of $\text{Bi}_2\text{O}_3 \cdot \text{MoO}_3$ has been studied in a fixed bed reactor under isothermal conditions (400°C). The propylene concentration at the reactor inlet was varied over the range 1.04–2.15 mmol/liter and the ammonia concentration over the range 0.78–1.71 mmol/liter. The oxygen consumption rate was found to be independent of the propylene and ammonia concentrations.

A quantitative kinetic model has been derived in which a surface reaction more or less inhibited by a product and oxygen diffusion through the lattice of the catalyst are combined. In this model a distinction is made between selective X-sites and nonselective Y-sites on the catalyst surface. The model provides a good description of the experimental results and also fits in with previous observations.

INTRODUCTION

The heterogeneous selective ammoxidation of propylene into acrylonitrile over mixed oxide catalysts has been intensively studied (1–4). Mostly bismuth molybdates have been used in these investigations and although the proposed reaction models differ in detail (5–9), possibly as a result of differences in experimental conditions, they all agree that the ammoxidation of propylene is a redox type of reaction. In this reaction the oxygen is supplied by the catalyst and subsequently the reduced catalyst is reoxidized, as has been suggested originally by Mars and van Krevelen (10). Although recent studies support the view that the lattice oxygen ions are very mobile (11,12), our results suggest that the oxygen diffusion process in combination with product inhibition is rate determining at 400°C.

¹ Present address: Shell Internationale Petroleum, Maatschappij, B.V.

LIST OF SYMBOLS

A	Acrolein concentration in the gas phase, mmole liter ⁻¹
C_1	$= \frac{DP_0^3 + EP_0^2 + 2FP_0}{DP_0^2 + F} \quad [\text{Eq. (6)}],$ mmole ³ liter ⁻³ gcat ⁻¹ min ⁻¹
C_2	$= \frac{2P_0^2}{DP_0^2 + F} \quad [\text{Eq. (6)}],$ mmole ³ liter ⁻³ gcat ⁻¹ min ⁻¹
C_3	$= \frac{DP_0^4 + 2EP_0^3 + 3FP_0^2}{DP_0^2 + F} \quad [\text{Eq. (6)}],$ mmole ³ liter ⁻³
D	$= \frac{s_A^2 K_A}{f_A k_{D_0}},$ liter ² gcat min mmole ⁻³
E	$= \frac{s_A}{f_A k_{D_0}} + \frac{s_A}{k_{r_A}},$ liter gcat min mmole ⁻²

$$F = \frac{s_A}{k_{rA}K_P}, \text{ gcat min mmole}^{-1}$$

$$G = \frac{2}{3f_Nk_{D_0}} + \frac{2}{3k_{rN}}, \text{ liter gcat min mmole}^{-2}$$

$$H = \frac{2s_AK_A}{3f_Nk_{D_0}}, \text{ mmole gcat}^{-1} \text{ min}^{-1}$$

f_A Fraction of the oxygen consumption used for acrolein formation

f_N Fraction of the oxygen consumption used for the nonselective nitrogen formation

k_{D_0} Oxygen diffusion coefficient, $\text{mmole}^2 \text{ liter}^{-1} \text{ gcat}^{-1} \text{ min}^{-1}$

k_{rA} Reaction rate coefficient of acrolein formation, $\text{mmole}^2 \text{ liter}^{-1} \text{ gcat}^{-1} \text{ min}^{-1}$

K_A Adsorption equilibrium constant for acrolein, liter mmole^{-1}

K_p Adsorption equilibrium constant for propylene, liter mmole^{-1}

N Total number of mmoles intake per minute, mmole min^{-1}

P Propylene concentration in the gas phase, mmole liter^{-1}

P_0 Propylene concentration in the gas phase at the reactor inlet, mmole liter^{-1}

s_A Selectivity of acrolein formation

θ_i Fraction of X-sites occupied by inhibiting acrolein

θ_N Fraction of X-sites occupied by ammonia

θ_{NP} Fraction of X-sites occupied by ammonia/propylene

θ_0 Fraction of X-sites occupied by ammonia and ammonia/propylene

θ_r Fraction of X-sites, reduced and not occupied by acrolein

W Amount of catalyst in the reactor, g

EXPERIMENTAL

The experiments have been carried out using propylene, ammonia, and "artificial

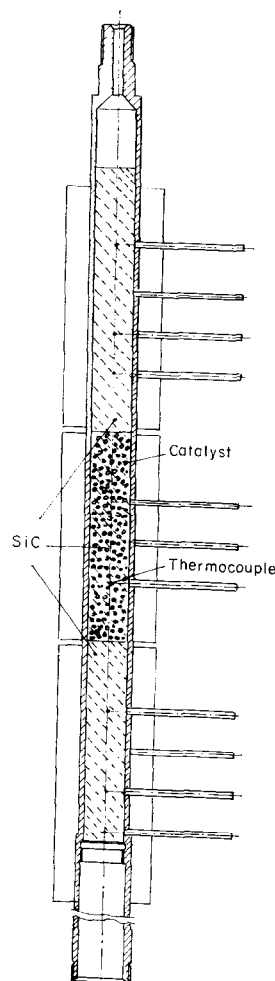


FIG. 1. Fixed bed reactor.

air" (a 20/80 oxygen/helium mixture). Besides these three streams, which were carefully controlled, an additional helium flow enabled us to adjust independently the inlet concentrations of each reactant. The stainless steel reactor, shown in Fig. 1, contains a fixed catalyst bed consisting of a mixture of unsupported koechlinite $\text{Bi}_2\text{O}_3 \cdot \text{MoO}_3$ and SiC. To keep the catalyst particles in their original position their diameter range is 1–2 mm, whereas that of the silicon carbide is 1–1.4 mm. During the filling of the catalyst in the reactor care has been taken to ensure an even distribution of the catalyst over the reactor volume.

As can be seen from Fig. 1, only the middle part of the reactor is filled with this diluted catalyst. The upper and lower part contain only SiC-particles. The axial temperature profile of the reactor bed is measured by means of eight chromel-alumel thermocouples at regular distances along the reactor. The reactor is surrounded by a cylindrical aluminum block which is divided into three sections which are heated independently. The temperature of the reactor is adjusted by controlling the wall temperature of the three sections. For all the experiments the temperature of the catalyst bed was kept at $400 \pm 1^\circ\text{C}$.

For each set of experiments with a constant feed consumption but increasing residence times, the flows of the reactants were maintained at a constant value, but an increasing fraction of the total reaction mixture was allowed to bypass the reactor.

The composition of the gas mixture was determined by gaschromatographic analysis. The gaseous products leaving the reactor flow into a thermostatted and manostattd sampling system with two eight-way sample valves in parallel. The reaction mixture from the reactor bypass can also be fed into the sampling system (see Fig. 2). After passing the sample loops the product stream is cooled, the liquid is collected in a cold trap, and the gaseous components are vented. The gaschromatographic analysis

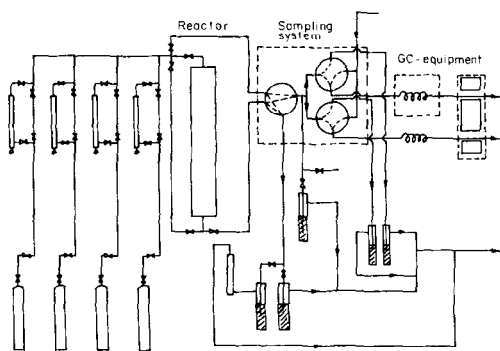


FIG. 2. Diagram of the apparatus used for the investigation of the kinetics of propylene ammoxidation.

TABLE 1
Experimental Conditions

Reaction temperature	400°C					
Pressure	79 cm Hg					
Volumetric flow	300-1200 scc/min					
Amount of catalyst	1.5 g Bi ₂ O ₃ ·MoO ₃					
Amount of dilution material	110 g SiC					
Concentrations at the reactor inlet (mmole/liter)						
C ₃ H ₆	1.51	1.51	1.55	1.04	1.49	2.15
NH ₃	0.78	1.14	1.71	1.19	1.19	1.19
O ₂	2.60	2.67	2.66	2.58	2.61	2.58

has been carried out with a two-column system. One column, containing Porapak Q and Porapak T, is used for the separation of carbon dioxide, propylene, ammonia, water, acetaldehyde, acrolein, acrylonitrile and acetonitrile. This separation requires temperature programming. A second column, which contains molecular sieve 13X, separates oxygen, nitrogen, and carbon monoxide at room temperature. In the dual katharometer system the carrier gas helium, flowing through one column, acts as a reference for the analysis carried out on the other column. Quantitative analysis of the effluent gas has been accomplished by integration of the various peak areas in conjunction with thermal conductivity response factors for the individual components.

The catalyst has been prepared according to the method of Batist and Lankhuyzen (13), and the experimental conditions are summarized in Table 1. In two experiments acrolein was added to the feed mixture, to check the inhibitory action of acrolein.

RESULTS

The conversion data are shown in Figs. 3 and 4, where reactant concentrations are given as a function of the contact time W/N .

In Fig. 3 the curves for propylene are almost parallel, indicating that the reaction

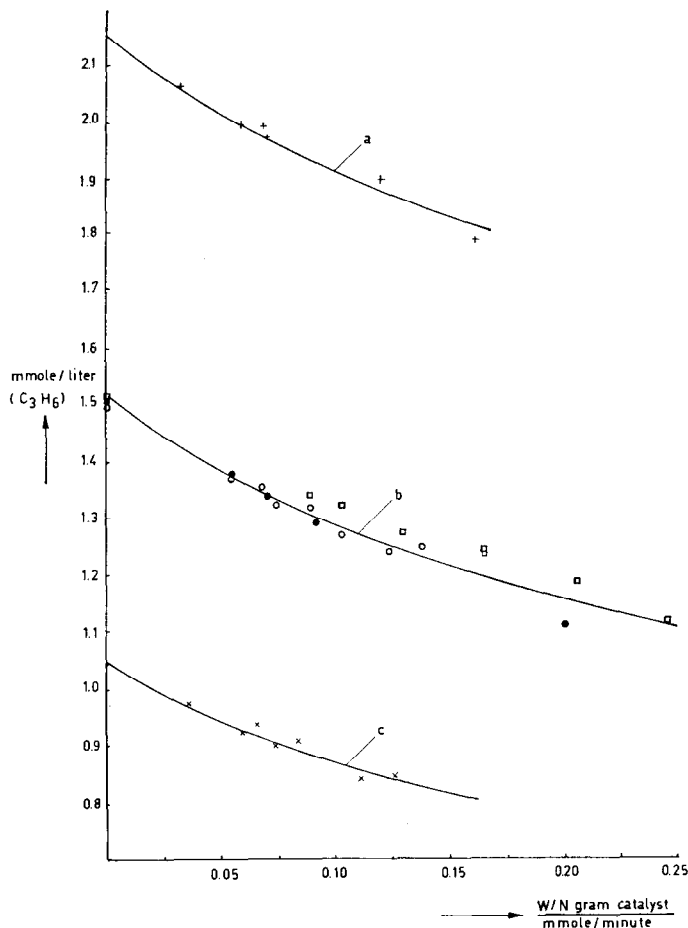


FIG. 3. Propylene concentration vs W/N . \bullet : $[C_3H_6]_0$, 1.51; $[NH_3]_0$, 0.78. \circ : $[C_3H_6]_0$, 1.51, $[NH_3]_0$, 1.14. \square : $[C_3H_6]_0$, 1.55; $[NH_3]_0$, 1.71. $+$: $[C_3H_6]_0$, 2.15; $[NH_3]_0$, 1.19. \times : $[C_3H_6]_0$, 1.04; $[NH_3]_0$, 1.19.

rate is almost zero order in the propylene concentration (from the initial slopes of the three curves one would calculate an order of about 0.25). A zero order, however, would require that the concentration curves be not only parallel, but also straight, which is not the case. Curve b of Fig. 3 in itself can quite accurately be described by $(-dP/d(W/N)) = 1.13P^{2.15}$ but this relation will not do at all for curves a and c.

Also, the influence of the ammonia concentration on the conversion rate of propylene is very small, as can be concluded from the data points belonging to curve b of Fig. 3. The curves for the ammonia con-

version are somewhat more complicated because at small contact times (W/N below 0.08 g cat min/mmol intake) part of the ammonia is oxidized to nitrogen. Therefore, we have in Fig. 4 (curves b, c, and d) at low contact times an ammonia conversion rate that is higher than the corresponding propylene conversion rate, whereas at higher contact times both rates are comparable. Curve a of Fig. 4 shows that the oxygen consumption as a function of the contact time is independent of the propylene and ammonia concentrations. Although the effect is less pronounced, the

same two regions as found for the ammonia conversion rate can be indicated here.

In Fig. 5 the acrylonitrile concentration is given as a function of the propylene consumption. From the linear relationship between the two, a constant selectivity of 0.80 follows. Similar linear functions have been found for carbon dioxide (selectivity 0.12) and acrolein (selectivity 0.08). As a result of the conversion initially of part of the ammonia into nitrogen the relationship between the acrylonitrile concentration and the ammonia consumption is less clear cut (Fig. 6). The data can be grouped some-

what according to the C_3H_6/NH_3 inlet ratio. This leads to a number of parallel straight lines. The slope of these lines is equivalent to an ultimate selectivity for ammonia of 0.80. When to an average mixture of propylene, ammonia, and oxygen, acrolein is added to a concentration of 0.55 mmol/liter the propylene conversion is reduced markedly. At a contact time $W/N = 0.15$ we found a reduction to less than 10% of the original value, and at a contact time of 0.09 the conversion was reduced to 15% of the original conversion at that contact time.

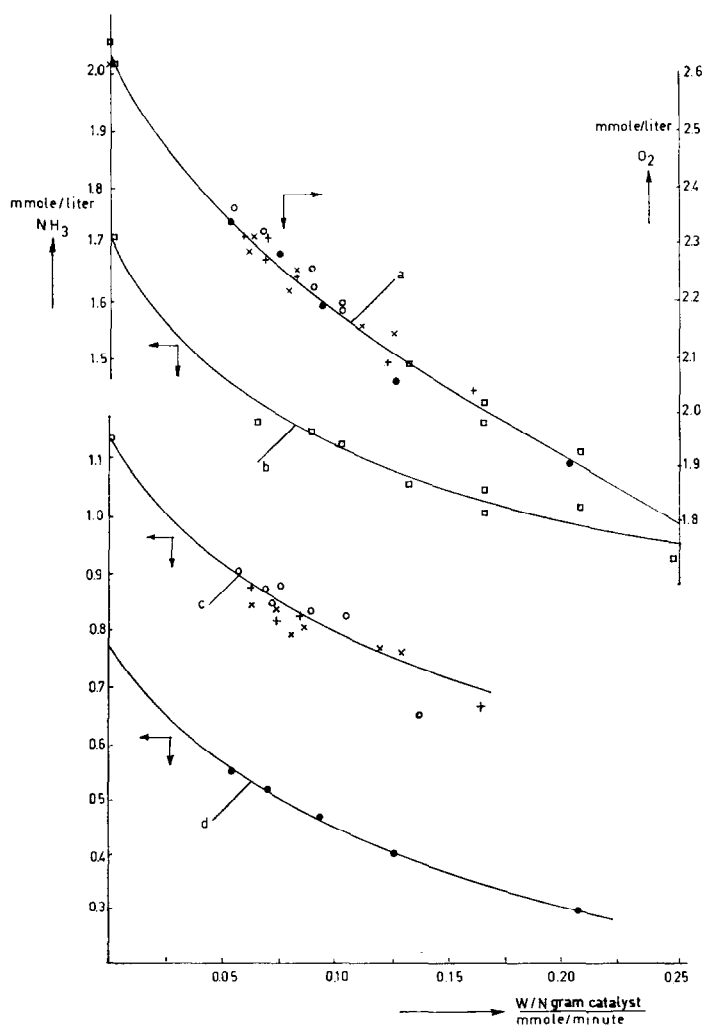


FIG. 4. Oxygen and ammonia concentrations vs W/N . For explanation of symbols see Fig. 3.

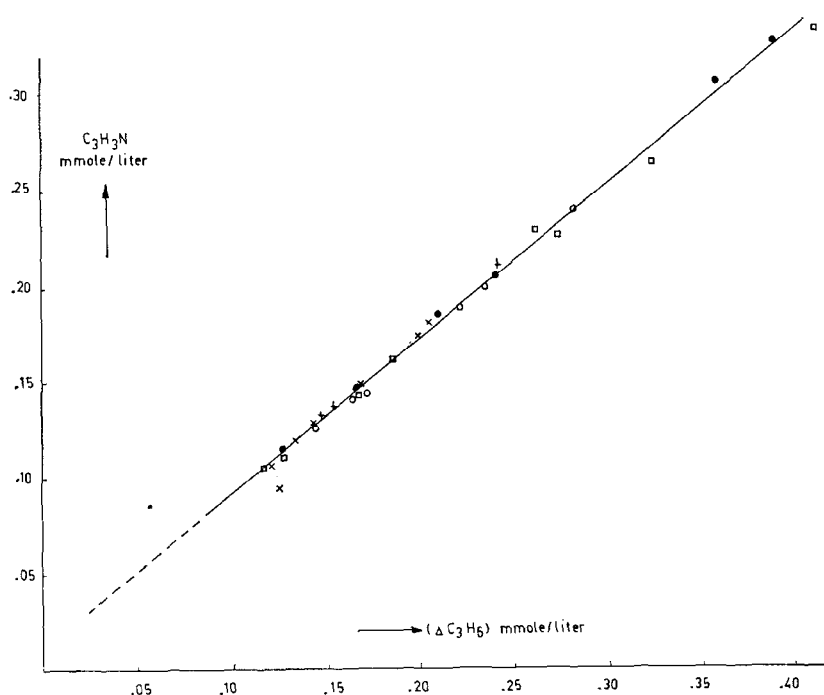


FIG. 5. Concentration of acrylonitrile vs decrease of the concentration of propylene. For explanation of symbols, see Fig. 3.

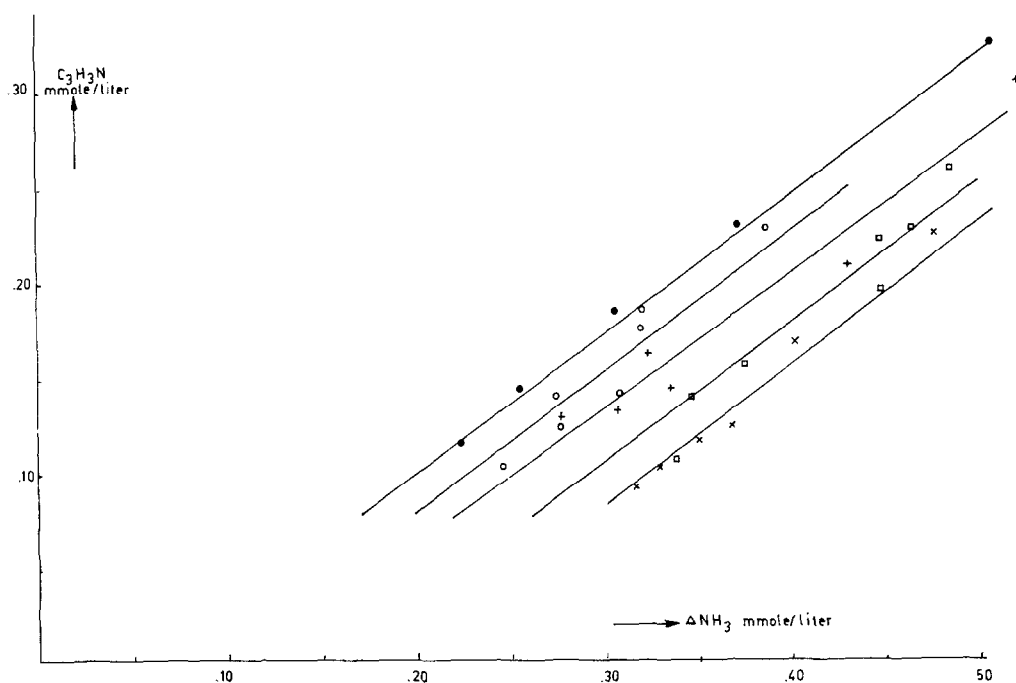


FIG. 6. Concentration of acrylonitrile vs decrease of the concentration of ammonia. For explanation of symbols see Fig. 3.

The above observations indicate the presence at the catalyst surface of two types of sites. There is one type of site (X-sites) on which 80% of the converted propylene and ammonia gives acrylonitrile. The remaining 20% of converted propylene divides into 12% for carbon dioxide and 8% for acrolein formation. The remaining 20% of converted ammonia yields nitrogen. The figures are not influenced by the variations in the initial propylene or ammonia concentrations that we have used in this investigation. From this we conclude that at these X-sites propylene and ammonia do not compete for adsorption and that the reaction sequence only starts after both a molecule of ammonia and one of propylene have been adsorbed. That one of every five propylene and ammonia molecules is not converted into acrylonitrile is either a stochastic phenomenon or is connected with small differences among the X-sites. On the other sites, the Y-sites, ammonia is oxidized nonselectively to nitrogen and water. These sites are rendered inactive rather quickly.

THE REACTION MODEL

In the following model we will mainly pay attention to the X-sites on which the propylene ammoxidation and oxidation reactions occur and give less consideration to the Y-sites on which the nonselective ammonia oxidation reaction takes place. The model is based on two assumptions:

(a) The oxygen is adsorbed at "catalyst reoxidation sites" and diffuses from there to the sites where the ammoxidation reaction takes place.

(b) A number of the latter sites are rendered inactive by the adsorption of acrolein.

The first assumption is in agreement with the oxygen isotope work of Keulks (12) and of Wragg, Ashmore, and Hockey (11). These investigations have shown that

the oxygen which takes part in the propylene oxidation comes from the lattice and not from the gas phase directly. Also, the work of Matsuura and Schuit (14,15) indicates that the reoxidation sites and the reaction sites are not the same. They find *inter alia* that the reoxidation rate of a partly reduced catalyst is not at all hampered by the presence of considerable quantities of hydrocarbon residues on the catalyst.

The second assumption is in agreement with the acrolein inhibition as described above. Experiments with steam as extra feed component did not show any inhibition and Cathala and Germain (2) did not find any influence of acrylonitrile itself on the conversion rate and selectivity of propylene in the ammoxidation reaction.

The model developed, however, would also hold for any other product inhibiting the reaction, provided that that product is also formed with a constant selectivity.

The model is in agreement with the diffusion model proposed by Batist *et al.* (8) and with the mechanistic adsorption model of Matsuura and Schuit (15,16). In terms of the latter model, two B-sites plus one A-site form one of our X-sites, whereas a Y-site corresponds to one of their A-sites in an isolated position.

According to these models reduction and reoxidation of the catalyst do not take place at the same sites. Therefore, diffusion of lattice oxygen must play a role. At the reduction side—the sites where the organic molecules react with the aid of lattice oxygen—the number of reactive X-sites can be divided into fractions θ_r , θ_i , and θ_0 (for explanation, see List of Symbols). On the oxidized sites ammonia adsorbs with a very fast reaction, resulting in complete occupancy and a reaction rate that is zero order in ammonia. However, before the reaction starts on these sites a molecule of propylene has to be adsorbed and as under our conditions the reaction rate has only a very low (0.25) order in propylene,

the propylene adsorption constant must have a rather high value. Consequently, $\theta_0 = \theta_N + \theta_{NP}$. At the oxidation side of the catalyst all sites are occupied by oxygen, according to the zero-order rate dependency of oxygen.

In the derivation of the expression for the rate of the propylene conversion we use the following equations. Adsorbed propylene is in equilibrium with propylene in the gas phase; thus,

$$\theta_{NP} = \theta_N K_p P. \quad (1)$$

The inhibition of acrolein is considered to be reversible and the adsorbed acrolein is in equilibrium with acrolein in the gas phase; thus,

$$\theta_i = \theta_r K_A A. \quad (2)$$

The selectivity of the acrolein formation is small but constant. Therefore, in the steady state the rate of oxygen diffusion, which is proportional to θ_r , is equal to the sum of the reaction rates and consequently, proportional to the rate of acrolein formation. Thus the following relation holds.

$$\theta_r = (k_{rA}/f_A k_{D0}) \theta_{NP}. \quad (3)$$

As

$$\theta_r + \theta_i + \theta_0 = 1, \quad (4)$$

we derive the equation for the propylene conversion rate,

$$\begin{aligned} \frac{dA}{dt} &= -s_A \frac{dP}{dt} \\ &= \frac{f_A k_{D0}}{1 + \frac{f_A k_{D0}}{k_{rA}} \left(\frac{1 + K_p P}{K_p P} \right) + K_A A}. \end{aligned} \quad (5)$$

After integration with $P = P_0$ at $t = W/N = 0$, we find by developing the logarithmic term in a Taylor series and neglecting the third and following terms

$$P = C_1 - (C_1^2 + C_2 t - C_3)^{1/2}. \quad (6)$$

Similar equations can be derived for oxygen and ammonia concentrations, caused by

reactions at the X-sites, as the ammonia selectivity at the X-sites is assumed to be constant.

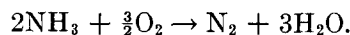
For the Y-sites we derive for the rate of the non-selective nitrogen formation, which is inhibited by acrolein formation correspondingly:

$$\frac{dN_2}{dt} = \frac{f_N k_{D0}}{1 + (f_N k_{D0}/k_{rN}) + K_A A}. \quad (7)$$

The rate of the oxygen consumption at the Y-sites then becomes

$$-\frac{dO_2}{dt_y} = \frac{\frac{3}{2} f_N k_{D0}}{1 + (f_N k_{D0}/k_{rN}) + K_A A}, \quad (8)$$

according to the reaction equation



Simplification of (8) at a given P_0 gives

$$r_{O_Y}^{-1} = G + H(P_0 - P). \quad (9)$$

The oxygen used at the Y-sites for the nonselective ammonia oxidation is the difference between the total oxygen consumption and the oxygen consumption at the X-sites. The latter can be calculated from the known selectivities at these sites. The validity of the model for the Y-sites is tested in Fig. 7, where it is shown that there exists a linear relationship between the propylene conversion at the X-sites and the reciprocal rate of the oxygen consumption at the Y-sites. This is in accordance with the prediction made in Eq. (9). The agreement between the experimental results and the model is shown in Fig. 3, where the curves are calculated according to (6). The constants C_1 , C_2 , and C_3 have been calculated with the following values for D , E , and F .

$$D = 1.232 \text{ liter}^2 \text{ g cat min/mmole}^3,$$

$$E = 0.162 \text{ liter g cat min/mmole}^2,$$

$$F = 0.305 \text{ g cat min/mmole}.$$

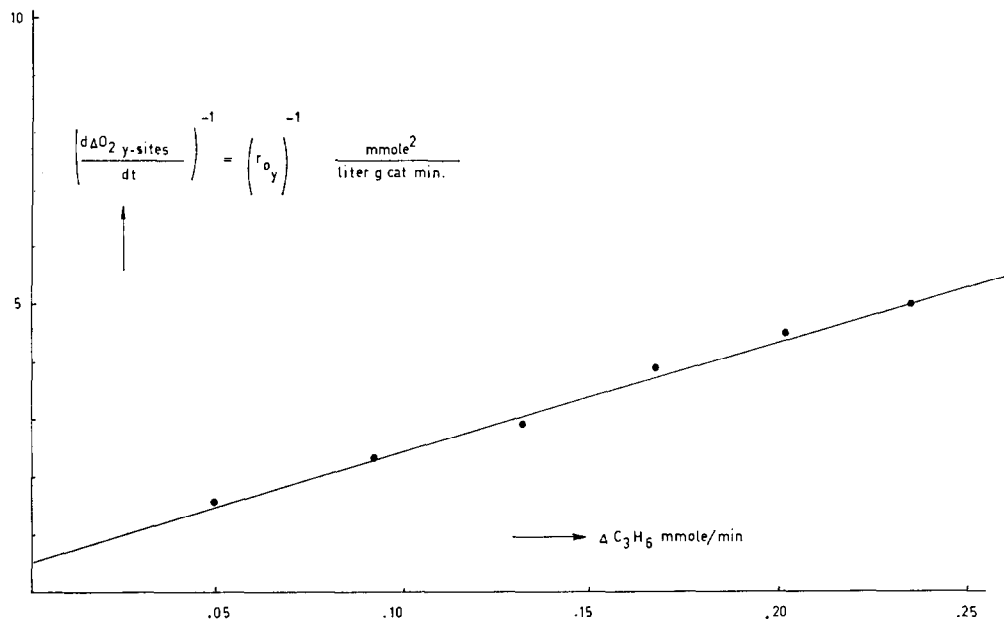


Fig. 7. Reciprocal rate of oxygen consumption by nonselective ammonia oxidation at the Y-sites vs decrease of the concentration of propylene.

ACKNOWLEDGMENT

The authors thank A. P. B. Sommen for carrying out some of the experiments and for analytical assistance.

REFERENCES

- Callahan, J. L., Grasselli, R. K., Milberger, E. C., and Strecker, H. A., *Ind. Eng. Chem. Prod. Res. Develop.* **9**, 134 (1970).
- Cathala, M., and Germain, J. E., *Bull. Soc. Chim. Fr.* 1970, 2167.
- Shelsted, K. A., and Chong, T. C., *Can. J. Chem. Eng.* **47**, 598 (1969).
- Pasquon, J., Trifiro, F., and Centola, P., *Chim. Ind. (Milan)* **49**, 1151 (1967).
- Aykan, K., *J. Catal.* **12**, 281 (1968).
- Berés, J., Brückman, K., Haber, J., and Janas, J., *Bull. Acad. Pol. Sci.* **20**, 8, 813 (1972).
- Cathala, M., Germain, J. E., *Bull. Soc. Chim. Fr.* 1970, 4114.
- Batist, Ph.A., der Kinderen, A. H. W. M., Leeuwenburgh, Y., Metz, F. A. M. G., and Schuit, G. C. A., *J. Catal.* **12**, 45 (1968).
- Wragg, R. D., Ashmore, P. G., and Hockey, J. A., *J. Catal.* **31**, 293 (1973).
- Mars, P., and van Krevelen, D. W., *Chem. Eng. Sci. Suppl.* **3**, 41 (1954).
- Wragg, R. D., Ashmore, P. G., and Hockey, J. A., *J. Catal.* **22**, 77 (1971).
- Keulks, G. W., *J. Catal.* **19**, 232 (1970).
- Batist, Ph. A., and Lankhuyzen, S. P., *J. Catal.* **28**, 496 (1973).
- Matsuura, I., and Schuit, G. C. A., *J. Catal.* **20**, 19 (1971).
- Matsuura, I., and Schuit, G. C. A., *J. Catal.* **25**, 314 (1972).
- Matsuura, I., *J. Catal.* **33**, 420 (1974).